

## X-irradiation of cells on glass slides has a dose doubling impact

Article (Accepted Version)

Kegel, Peter, Riballo, Enriqueta, Kühne, Martin, Jeggo, Penny and Löbrich, Markus (2007) X-irradiation of cells on glass slides has a dose doubling impact. *DNA Repair*, 6 (11). pp. 1692-1697. ISSN 1568-7864

This version is available from Sussex Research Online: <http://sro.sussex.ac.uk/id/eprint/1853/>

This document is made available in accordance with publisher policies and may differ from the published version or from the version of record. If you wish to cite this item you are advised to consult the publisher's version. Please see the URL above for details on accessing the published version.

### **Copyright and reuse:**

Sussex Research Online is a digital repository of the research output of the University.

Copyright and all moral rights to the version of the paper presented here belong to the individual author(s) and/or other copyright owners. To the extent reasonable and practicable, the material made available in SRO has been checked for eligibility before being made available.

Copies of full text items generally can be reproduced, displayed or performed and given to third parties in any format or medium for personal research or study, educational, or not-for-profit purposes without prior permission or charge, provided that the authors, title and full bibliographic details are credited, a hyperlink and/or URL is given for the original metadata page and the content is not changed in any way.

# **X-irradiation of cells on glass slides has a dose doubling impact**

Peter Kegel<sup>a</sup>, Enriqueta Riballo<sup>b</sup>, Martin Kühne<sup>a,c</sup>, Penny A. Jeggo<sup>b,\*</sup>, Markus Löbrich<sup>a,\*</sup>

<sup>a</sup>Fachrichtung Biophysik, Universität des Saarlandes, 66421 Homburg/Saar, Germany

<sup>b</sup>Genome Damage and Stability Centre, University of Sussex, East Sussex, BN1 9RQ, UK

\*Corresponding authors. Tel. +44-1273-678482; fax +44-1273-678121 (P. Jeggo). Tel. +49-6841-1626202; fax +49-6841-1626160 (M. Löbrich)

E-mail addresses: p.a.jeggo@sussex.ac.uk (P. Jeggo), markus.loebrich@uniklinik-saarland.de (M. Löbrich).

<sup>c</sup>Present address: Klinik für Strahlentherapie und Radioonkologie, Universität des Saarlandes, 66421 Homburg/Saar, Germany

## Abstract

Immunofluorescence detection of  $\gamma$ H2AX foci is a widely used tool to quantify the induction and repair of DNA double-strand breaks induced by ionising radiation. We observed that X-irradiation of mammalian cells exposed on glass slides induced 2-fold higher foci numbers compared to irradiation with  $\gamma$ -rays. Here, we show that the excess  $\gamma$ H2AX foci after X-irradiation are produced from secondary radiation particles generated from the irradiation of glass slides. Both 120 kV X-rays and  $^{137}\text{Cs}$   $\gamma$ -rays induce  $\sim 20$   $\gamma$ H2AX foci per Gy in cells growing on thin ( $\sim 2$   $\mu\text{m}$ ) plastic foils immersed in water. The same yield is obtained following  $\gamma$ -irradiation of cells growing on glass slides. However, 120 kV X-rays produce  $\sim 40$   $\gamma$ H2AX foci per Gy in cells growing on glass, two-fold greater than obtained using cells irradiated on plastic surfaces. The same increase in  $\gamma$ H2AX foci number is obtained if the plastic foil on which the cells are grown is irradiated on a glass slide. Thus, the physical proximity to the glass material and not morphological differences of cells growing on different surfaces accounts for the excess  $\gamma$ H2AX foci. The increase in foci number depends on the energy and is considerably smaller for 25 kV relative to 120 kV X-rays, a finding which can be explained by known physical properties of radiation. The kinetics for the loss of foci, which is taken to represent the rate of DSB repair, as well as the Artemis dependent repair fraction, was similar following X- or  $\gamma$ -irradiation, demonstrating that DSBs induced by this range of treatments are repaired in an identical manner.

## Introduction

DNA double-strand breaks (DSBs) represent important lesions determining most of the deleterious effects of ionising irradiation (IR). The induction of DSBs is linearly dependent on the radiation dose with typical yields determined by pulsed-field gel electrophoresis (PFGE) being between 5 and 6 DSBs per Gbp per Gy for photon irradiation (summarized in (1)). This corresponds to about 30-36 DSBs per Gy for a G1 phase diploid human cell. Recently,  $\gamma$ H2AX foci analysis has become a widely used tool to quantify DSBs on a single cell level after IR (2).  $\gamma$ H2AX foci numbers of 30-35 per Gy per G1 cell have been reported (3-8) suggesting that there is a 1:1 correlation between  $\gamma$ H2AX foci and DSBs after IR of non-replicating cells. However, the precise DSB induction yields following irradiation can depend on a number of factors (see, eg, (9)) and, we show here, are critically dependent upon the surface upon which the cells are grown and irradiated.

When photon radiation interacts with matter, secondary electrons can be emitted by either the photo-electric or Compton effect. The majority of DSBs after IR are produced by such secondary electrons at sites distant to the original photon track. For photon energies below  $\sim 60$  keV, the photo-electric effect is the predominant process generating secondary electrons with energies similar to the original photon energy (10). The number of electrons generated due to this process is strongly dependent on the atomic number,  $Z$ , of the irradiated matter (proportional to the fourth power of  $Z$ ). Hence, irradiation of material with high  $Z$  generates many more secondary electrons than irradiating low- $Z$  material, and low- $Z$  material can receive additional energy which is deposited by secondary electrons generated in nearby material with high  $Z$ . The range of the secondary electrons varies from  $\sim 2$   $\mu\text{m}$  for 10 keV electrons to  $\sim 100$   $\mu\text{m}$  for 100 keV electrons and determines the size of the area surrounding high- $Z$  material in which additional energy is deposited ((11) and references therein). Thus, cells X-irradiated with photon energies of  $\sim 60$  keV (eg X-rays) may receive a higher dose if material with high  $Z$  is present within a few tens of micrometers. Typical dosimetric procedures employ conditions representing a cell surrounded by tissue or aqueous material, such as a tissue-equivalent gas in an ion-chamber or an aqueous solution. Hence, standard dosimetry estimations likely underestimate the dose received by cells X-irradiated in close proximity to high- $Z$  material. Above photon energies of  $\sim 60$  keV, the Compton effect represents the main interaction process for photon radiation with matter. The deposited energy per mass (ie the dose) due to this process is essentially independent of  $Z$ . Hence, cells irradiated with photon energies considerably higher than 60 keV (eg  $\gamma$ -rays) are unlikely to be influenced by the close proximity of high- $Z$  material.

Most of the procedures for  $\gamma$ H2AX foci analysis involve the irradiation of cells growing as monolayers on glass coverslips. This contrasts to most other techniques for measuring DSBs, eg PFGE, and, indeed, most other cellular analysis, which utilise cells irradiated in plastic cell culture flasks or dishes. The atomic composition of glass involves a significant contribution of Silicium with an atomic number Z of 14. This raises the possibility that cells X-irradiated on a glass surface during  $\gamma$ H2AX foci analysis receive a higher dose than estimated via standard dosimetry measurements. Here, we compare  $\gamma$ H2AX foci numbers in cells growing on different surfaces and demonstrate that irradiating cells on glass surfaces with 25 or 120 kV X-rays (representing photon energy distributions with intensity maxima of ~15 and ~60 keV, respectively) leads to a considerable increase in foci numbers compared with irradiation conditions on plastic surfaces or on water. This is an important consideration for cellular biologists exploiting radiation to examine DNA damage response mechanisms. Thus, caution should be taken when comparing DSB induction and repair by  $\gamma$ H2AX foci analysis following X-irradiation on glass coverslips with other cellular responses examined using techniques that involve growth of cells on plastic surfaces, such as FACs analysis, Western Blotting, and cell survival studies.

Additionally, we exploited the exquisitely sensitive  $\gamma$ H2AX foci assay to monitor parameters of repair following X- or  $\gamma$ -irradiation. Our results show that DSBs induced by photon energies ranging from 15 to 660 keV are repaired with similar kinetics and have a similar dependency upon Artemis and ATM for their repair.

## Materials and Methods

### *Cell culture*

Primary human fibroblasts MRC-5 (wild-type, European Collection of Animal Cell Cultures no. 84101801), HSF1 (wild-type, kindly provided by H.P. Rodemann, University of Tübingen, Tübingen, Germany), 180BR (hypomorphic for DNA ligase IV (12)), CJ179 and F01-240 (both deficient for Artemis (7)), and hTert immortalized derivatives, 48BRhTert (wild-type, Medical Research Council, Brighton, UK) and CJ179hTert were grown in minimal essential medium (Biochrom) supplemented with 10% (MRC-5, HSF1, 48 hTert, CJ179 hTert) or 20% (180BR, CJ179, F01-240) FCS, non-essential amino acids and antibiotics. Cells were grown and irradiated on ~0.2 mm glass coverslips (primary fibroblasts: D263M, Schott Desag AG, Grünenplan, Germany; hTert immortalized fibroblasts: GNCS 102222, G&N Ltd, Billingshurst, West Sussex, UK) or on ~2 µm mylar foil which formed the bottom of cylindrical plastic rings (13). All experiments were performed with nondividing confluent cultures with at least 95% of the cells in G1, as determined by flow cytometry in pilot experiments.

### *Irradiation and dosimetry*

Primary fibroblasts were irradiated in cell culture medium at room temperature. X-irradiation at 25 or 120 kV was performed using a Phillips PW2184 or a Müller MÖD 150Be X-ray machine, respectively, both equipped with tungsten anode and a thin (<0.2 mm) beryllium window. Samples were positioned at a distance of ~30 cm above the beryllium window. For the 120 kV setting, a 9 mm aluminum plate directly positioned above the window and a 1 mm aluminum plate holding the samples were used for filtering. This setup provided an X-ray bremsstrahlung-spectrum with photon energies from ~30 to 120 keV and a predominant characteristic X-ray peak at ~60 keV (14). For the 25 kV setting, only a plate holding the samples (0.5 mm aluminum) was used, providing a bremsstrahlung-spectrum from ~8 to 25 keV with an intensity maximum at ~15 keV and no significant characteristic X-ray peak (15). The dose rates were ~0.5 Gy/min and ~1 Gy/min for the 25 and 120 kV settings, respectively.  $\gamma$ -irradiation with an energy of 660 keV was performed using a  $^{137}\text{Cs}$  source oscillating vertically. Samples were placed at a distance of ~30 cm from the source and were rotated during irradiation. The setup provided a dose rate of ~3.5 Gy/min without any significant filtering. Fricke dosimetry was performed for 120 kV X-irradiation and  $^{137}\text{Cs}$   $\gamma$ -irradiation. Physical dosimetry was performed for the two X-ray energies. An ion chamber for photon energies from 7.5 to 100 keV (SN4, M23342-751; PTW Freiburg, Freiburg, Germany) was used for both 25 and 120 kV X-rays. Additionally, an ion chamber for energies above 70 keV

(SN4, M23331-453; PTW Freiburg, Freiburg, Germany) was utilized for the 120 kV X-rays. For the 120 kV X-rays, results from both ion chambers and from Fricke dosimetry were identical within ~10%, demonstrating that the different procedures provide similar results.

hTert immortalized fibroblasts were X-irradiated at 120 kV using a Comet MXR-320/26 X-ray machine with tungsten anode, beryllium window and 1 mm aluminum filtering. Samples were placed at a distance of 65 cm from the window and irradiated at a dose rate of ~0.5 Gy/min.  $\gamma$ -irradiation was performed using a  $^{137}\text{Cs}$  source (Gammacell 1000, Atomic Energy of Canada Ltd). Samples were rotated during irradiation at a dose rate of ~8.5 Gy/min.

### *Immunofluorescence*

Primary fibroblasts were fixed in 2% paraformaldehyde for 15 min, washed in PBS for 3 x 10 min, permeabilized for 5 min on ice in 0.2% Triton X-100 in 1% FCS in PBS, and blocked with 1% FCS in PBS for 3 x 10 min at room temperature. Samples were incubated with anti- $\gamma\text{H2AX}$  monoclonal antibody (1:200; Upstate, Charlottesville, VA) in 1% FCS in PBS for 1 h, washed in 1% FCS in PBS for 3 x 10 min, and incubated with Alexa Fluor 488-conjugated goat anti-mouse secondary antibody (1:500; Molecular Probes, Eugene, OR) in 1% FCS in PBS for 1 h at room temperature. Cells were washed in PBS for 4 x 10 min and mounted using Vectashield mounting medium with 0.000025% 4,6 diamino-2-phenylindole (Vector Laboratories, Burlingame, CA). Foci were counted by eye during the imaging process using a x63 objective on a Zeiss Axioplan 2 imaging epifluorescent microscope equipped with ISIS software (MetaSystems, Altlußheim, Germany). In a single experiment, at least 40 cells were analysed per sample.

hTert immortalized fibroblasts were fixed in 2% paraformaldehyde, 2% sucrose in PBS for 10 min at room temperature and permeabilized in 0.2% Triton X-100 in PBS for 2 min. Samples were incubated with anti- $\gamma\text{H2AX}$  monoclonal antibody (1:800; Upstate, Charlottesville, VA) in 2% bovine albumin fraction V in PBS for 30 min at 37°C, washed with PBS for 3 x 10 min, incubated with FITC-conjugated goat anti-mouse secondary antibody (1:200; Molecular Probes, Eugene, OR) in 2% bovine albumin fraction V in PBS for 30 min at 37°C, and again washed with PBS for 3 x 10 min. Nuclei were counterstained with 4,6 diamino-2-phenylindole (0.000025% in PBS) for 10 min, mounted using Vectashield mounting medium (Vector Laboratories, Burlingame, CA) and examined using a Leitz DIAPLAN x100 objective.

## Results and Discussion

Previous comparison of  $\gamma$ H2AX foci numbers obtained from our two laboratories suggested a marked difference in the initial yield as well as in the level of foci remaining at defined times post irradiation (see, eg, reference 7 and data not shown). The evaluation of the same samples by both laboratories using different microscopic systems excluded the possibility that different scoring conditions could account for different foci numbers. Hence, we considered the possibility that the different radiation qualities used in our two laboratories (mainly  $\gamma$ -rays in the PAJ lab and X-rays in the ML lab) produce different foci numbers and undertook a systematic study to address this.

We irradiated parallel samples of primary human fibroblasts grown on glass coverslips to confluency with varying doses of 25 kV X-rays, 120 kV X-rays or  $^{137}\text{Cs}$   $\gamma$ -rays and scored  $\gamma$ H2AX foci at 15 min post irradiation (Fig. 1). Remarkably, we observed an approximately two-fold higher yield of foci per cell after 120 kV X-irradiation than after  $\gamma$ -irradiation (~40 foci per Gy vs. ~20 foci per Gy). 25 kV X-rays produced ~20% less foci than 120 kV X-rays (Fig. 1). Such a significant difference between X- and  $\gamma$ -rays was highly surprising but reproduced consistently in both laboratories (data not shown). However, it is difficult to reconcile the difference in foci numbers between X- and  $\gamma$ -rays with their similar physical properties, and experiments using PFGE with cells irradiated in flasks failed to reveal a similar pronounced difference in DSB yields (see reference (1) for a summary of many data sets).

In the course of a different study, we observed that the yield of  $\gamma$ H2AX foci in lymphocytes irradiated in suspension with 120 kV X-rays increases substantially when contrast medium was added prior to irradiation. Contrast medium has a high atomic number, Z, and is used during radiodiagnostic procedures to increase energy absorption. Elevated  $\gamma$ H2AX foci numbers were not observed if the contrast medium was added immediately after irradiation, ie it has to be present at the time of irradiation. Remarkably, contrast medium does not enhance the foci yield for  $\gamma$ -rays, whose main interaction process is the Compton effect and for which no increase in dose would be expected (manuscript in preparation).

We, therefore, examined whether the higher foci numbers for X-rays compared with  $\gamma$ -rays following irradiation of cells on glass coverslips might reflect excess radiation damage generated by secondary electrons originating from the glass material. We irradiated cells growing on thin (2  $\mu\text{m}$ ) plastic foils with 25 kV X-rays, 120 kV X-rays or  $^{137}\text{Cs}$   $\gamma$ -rays (Fig. 2). Strikingly, when the plastic foil was positioned on a plastic dish during irradiation, all three radiation qualities produced the same foci yield (~20 foci per Gy), which was also



similar to the yield after  $\gamma$ -irradiation of cells on glass. The similar yield for  $\gamma$ -rays suggests that different morphological features for cells growing on different surfaces are unlikely to account for the elevated foci numbers for cells X-irradiated on glass. To provide further evidence for the notion that proximity to the glass material can increase the radiation damage, we placed the thin plastic foils containing the cells on top of a glass slide during irradiation. We observed increased foci numbers after 120 kV X-irradiation similar to that observed for cells growing on glass, ie an increase from 20 per cell per Gy to 40 per cell per Gy if a glass slide is placed directly underneath the plastic foil without being in contact with the cells (Fig. 2). Interestingly, no increase in foci number due to the proximity of glass material was observed for 25 kV X-rays consistent with the notion that most electrons generated by 25 kV X-rays have energies of  $\sim 15$  keV and a maximum range in water of  $\sim 3$   $\mu\text{m}$  and, hence, are unlikely to penetrate the foil, the cell cytoplasm and reach the cell nucleus. A considerable elevation in foci number after 120 kV X-irradiation is also observed if an Aluminum plate ( $Z=13$ ) is positioned directly underneath the plastic foil, suggesting that other high-Z material can produce a similar effect. Finally, we examined the induction of  $\gamma\text{H2AX}$  foci in cells under conditions closely resembling their natural cellular environment by placing cells growing on the thin plastic foils onto a water surface during irradiation. About 20 foci per Gy per cell were observed for 25 kV X-rays, 120 kV X-rays and  $^{137}\text{Cs}$   $\gamma$ -rays.

We routinely estimate DSB induction by monitoring the yield of  $\gamma\text{H2AX}$  foci 15 min post irradiation since at this time the foci have grown to a size which is suitable for reliable quantification. However, as we have shown previously some DSB repair can occur during the first 15 min post irradiation and foci numbers assessed at 3 min post irradiation are  $\sim 20$ -40% higher (5). Hence, initial foci numbers suggest that  $\sim 25$  foci are formed per Gy per cell. This is slightly lower than the reported 30-36 DSBs per Gy per cell assessed by PFGE analysis (1). It is possible that  $\gamma\text{H2AX}$  foci analysis may underestimate DSB formation. Alternatively, the PFGE technique may overestimate the initial number of DSBs as heat-labile sites produced by IR can be transformed into DSBs during the lysis step of PFGE (16).

We next sought to compare the rate of DSB repair for the three conditions, namely 25 and 120 kV X- and  $^{137}\text{Cs}$   $\gamma$ -irradiation on glass coverslips (Figs. 3 and 4). The results demonstrate that all three radiation conditions induced  $\gamma\text{H2AX}$  foci that were repaired with the same kinetics both in DSB repair-proficient wild-type cells and in repair-deficient cells hypomorphic for DNA ligase IV. Moreover, all had a similar fraction of foci that required ATM and Artemis for their repair. 50% of the foci induced by 120 kV X-rays are derived from irradiation of the glass material. However, the repair kinetics was identical to that observed for 25 kV X- and  $\gamma$ -rays. Firstly, this verifies that the excess  $\gamma\text{H2AX}$  foci are

induced via the mechanism described, ie by secondary electrons, and represent DSBs. Secondly, our findings suggest that DSBs induced by photon energies ranging from 15 to 660 keV are repaired with similar kinetics and thus, we assume are of similar complexity. This is important for allowing the comparison of rates of repair between laboratories, who may use different radiation sources and radiation conditions. Another important factor which can influence the energy of the radiation applied is the use of filtering devices. This may vary between radiation sources and may also affect the yield of DSBs. Our findings would suggest that whilst this may influence the DSB yield, it is unlikely to impact significantly on either the rate of repair or the magnitude of the Artemis dependent fraction. Indeed, a similar Artemis dependent fraction has been observed in different laboratories despite the different radiation conditions used (7, 17, 18, 19).

In summary, we have shown that cells X-irradiated on glass slides exhibit an excess of DSBs which are produced by secondary electrons generated from the irradiation of the glass material. Thus, the dose received by a cell X-irradiated on glass can be considerably higher than suggested by standard dosimetry measurements. Indeed, the dose was two-fold higher for cells irradiated with 120 kV X-rays on glass compared to irradiation on plastic surfaces. The elevation in foci number is not observed for  $\gamma$ -rays. This difference can be explained by known physical parameters of radiation. Given the increased sensitivity of biological assays to monitor DNA damage, it is important for biologists exploiting radiation as a DNA damaging agent to consider these physical attributes of radiation not only when comparing findings between laboratories but even within a laboratory if different surfaces are employed. However, we show that the kinetics for DSB repair are unaffected by the increase in dose as the extra DSBs arising appear to be of a similar complexity, and are repaired at a similar rate.

### **Acknowledgements**

The ML laboratory is supported by the Deutsche Forschungsgemeinschaft (Grant LO 677/4-1/2), the Bundesministerium für Bildung und Forschung via the Forschungszentrum Karlsruhe (Grants 02S8132 and 02S8335), the Deutsche Zentrum für Luft und Raumfahrt e.V. (Grant 50WB0017), the Gesellschaft für Schwerionenforschung Darmstadt (Grant HO-LOEB), and the Wilhelm Sander-Stiftung (Grant 2003.114.1/3). The PAJ laboratory is supported by the Medical Research Council, the Human Frontiers Science Programme, the Association for International Cancer Research and the Leukaemia Research Fund. Both laboratories are supported by EU grant FI6R-CT-2003-508842 (RiscRad).

## References

1. K.M. Prise, G. Ahnstrom, M. Belli, J. Carlsson, D. Frankenberg, J. Kiefer, M. Löbrich, B.D. Michael, J. Nygren, G. Simone, B. Stenerlow, A review of dsb induction data for varying quality radiations, *Int. J. Radiat. Biol.* 74 (1998) 173-184.
2. E.P. Rogakou, C. Boon, C. Redon, W.M. Bonner, Megabase chromatin domains involved in DNA double-strand breaks in vivo, *J. Cell Biol.* 146 (1999) 905-916.
3. K. Rothkamm, M. Löbrich, Evidence for a lack of DNA double-strand break repair in human cells exposed to very low x-ray doses, *Proc. Natl. Acad. Sci. USA* 100 (2003) 5057-5062.
4. M. Löbrich, P.A. Jeggo, Harmonising the response to DSBs: a new string in the ATM bow, *DNA Repair* 4 (2005) 749-759.
5. M. Kühne, E. Riballo, N. Rief, K. Rothkamm, P.A. Jeggo, M. Löbrich, A double-strand break repair defect in ATM-deficient cells contributes to radiosensitivity, *Cancer Res.* 64 (2004) 500-508.
6. M. Löbrich, N. Rief, M. Kühne, M. Heckmann, J. Fleckenstein, C. Rube, M. Uder, In vivo formation and repair of DNA double-strand breaks after computed tomography examinations, *Proc. Natl. Acad. Sci. USA* 102 (2005) 8984-8989.
7. E. Riballo, M. Kühne, N. Rief, A. Doherty, G.C. Smith, M.J. Recio, C. Reis, K. Dahm, A. Fricke, A. Krempler, A.R. Parker, S.P. Jackson, A. Gennery, P.A. Jeggo, M. Löbrich, A pathway of double-strand break rejoining dependent upon ATM, Artemis, and proteins locating to gamma-H2AX foci, *Mol. Cell* 16 (2004) 715-724.
8. S.H. MacPhail, J.P. Banath, T.Y. Yu, E.H. Chu, H. Lambur, P.L. Olive, Expression of phosphorylated histone H2AX in cultured cell lines following exposure to X-rays, *Int. J. Radiat. Biol.* 79 (2003) 351-358.
9. H. Nikjoo, P. O'Neill, W.E. Wilson, D.T. Goodhead, Computational approach for determining the spectrum of DNA damage induced by ionizing radiation, *Radiat. Res.* 156 (2001) 577-583.
10. A. Kellerer, Electron spectra and the RBE of X rays, *Radiat. Res.* 158 (2002) 13-22.
11. J. Meesungnoen, J.P. Jay-Gerin, A. Filali-Mouhim, S. Mankhetkorn, Low-energy electron penetration range in liquid water, *Radiat. Res.* 158 (2002) 657-660.
12. E. Riballo, S.E. Critchlow, S.H. Teo, A.J. Doherty, A. Priestley, B. Broughton, B. Kysela, H. Beamish, N. Plowman, C.F. Arlett, A.R. Lehmann, S.P. Jackson, P.A. Jeggo, Identification of a defect in DNA ligase IV in a radiosensitive leukaemia patient, *Curr. Biol.* 9 (1999) 699-702.

13. M. Kühne, K. Rothkamm, M. Löbrich, No dose-dependence of DNA double-strand break misrejoining following alpha-particle irradiation, *Int. J. Radiat. Biol.* 76 (2000) 891-900.
14. R. Birch, M. Marshall, Computation of Bremsstrahlung X-ray spectra and comparison with spectra measured with a Ge(Li) detector, *Phys. Med. Biol.* 24 (1979) 505-517.
15. E.A. Burke, R.M. Pettit. Absorption analysis of X-ray spectra produced by beryllium window tubes operated at 20 to 50 Kvp. *Radiat. Res.* 13 (1960) 271-285.
16. B. Rydberg, Radiation-induced heat-labile sites that convert into DNA double-strand breaks, *Radiat. Res.* 153 (2000) 805-812.
17. J. Wang, J.M. Pluth, P.K. Cooper, M.J. Cowan, D.J. Chen, S.M. Yannone, Artemis deficiency confers a DNA double-strand break repair defect and Artemis phosphorylation status is altered by DNA damage and cell cycle progression, *DNA Repair* 4 (2005) 556-570.
18. D. Deckbar, J. Birraux, A. Krempler, L. Tchouandong, A. Beucher, S. Walker, T. Stiff, P. Jeggo, M. Löbrich, Chromosome breakage after G2 checkpoint release, *J Cell Biol.* 176 (2007) 749-755.
19. F. Darroudi, W. Wiegant, M. Meijers, A.A. Friedl, M. van der Burg, J. Fomina, J.J. van Dongen, D.C. van Gent, M.Z. Zdzienicka, Role of Artemis in DSB repair and guarding chromosomal stability following exposure to ionizing radiation at different stages of cell cycle, *Mutat Res.* 615 (2007) 111-124.

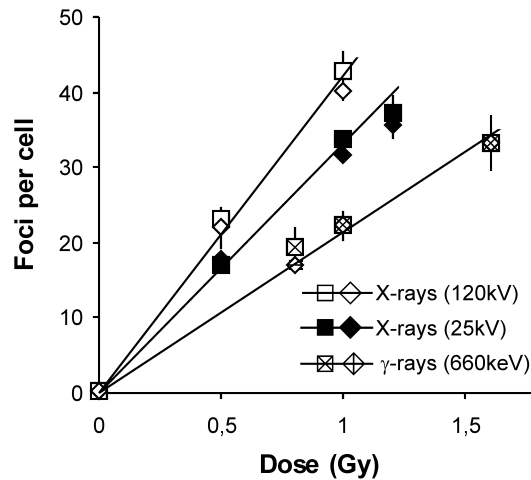


Fig. 1:  $\gamma$ H2AX foci assessed at 15 min post irradiation in primary human fibroblasts (squares: HSF1 cells; diamonds: CJ179 cells). The cells were grown and irradiated on glass coverslips immersed in cell culture medium inside a plastic dish. All three radiation qualities produced foci numbers proportional to dose (25 kV X-rays: 33 foci/cell/Gy; 120 kV X-rays: 41 foci/cell/Gy;  $\gamma$ -rays: 21 foci/cell/Gy; derived from a linear fit to the data from both cell lines). Note that non-linear relationships between foci and dose were observed for foci numbers greater than ~50 foci per cell, probably reflecting difficulties in scoring high foci numbers (data not shown). Error bars represent the SE from at least 3 independent experiments.

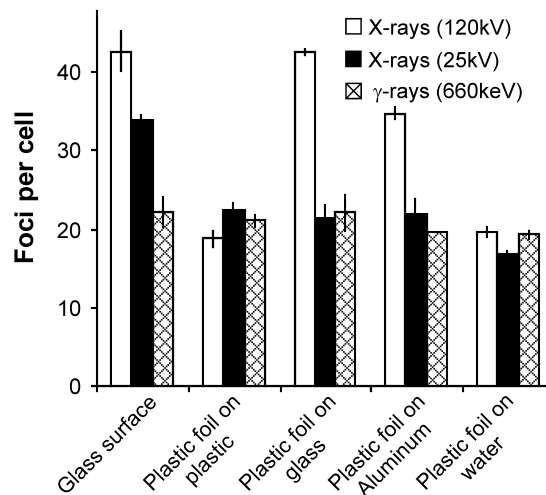


Fig. 2:  $\gamma$ H2AX foci assessed at 15 min post irradiation with 1 Gy in primary human fibroblasts (MRC-5 cells). The cells were either grown and irradiated on glass coverslips as for Fig. 1 (left group of columns) or were grown and irradiated on thin plastic foils which represented to bottom of a plastic ring (remaining four groups). The foils carrying the cells on top were placed onto different materials during irradiation: onto a plastic dish, a glass coverslip, a thin (2 mm) aluminum plate or a thin (5 mm) water layer. For all irradiations, cell culture medium was present in the plastic ring to prevent cells becoming dry. Irradiation was delivered from the bottom, ie photons had to penetrate the different materials at the bottom of the plastic foil, then the foil and then reached the cells. Control experiments had shown that the different materials did not shield the radiation to any measurable extent (data not shown). Error bars represent the SE from at least 3 independent experiments.

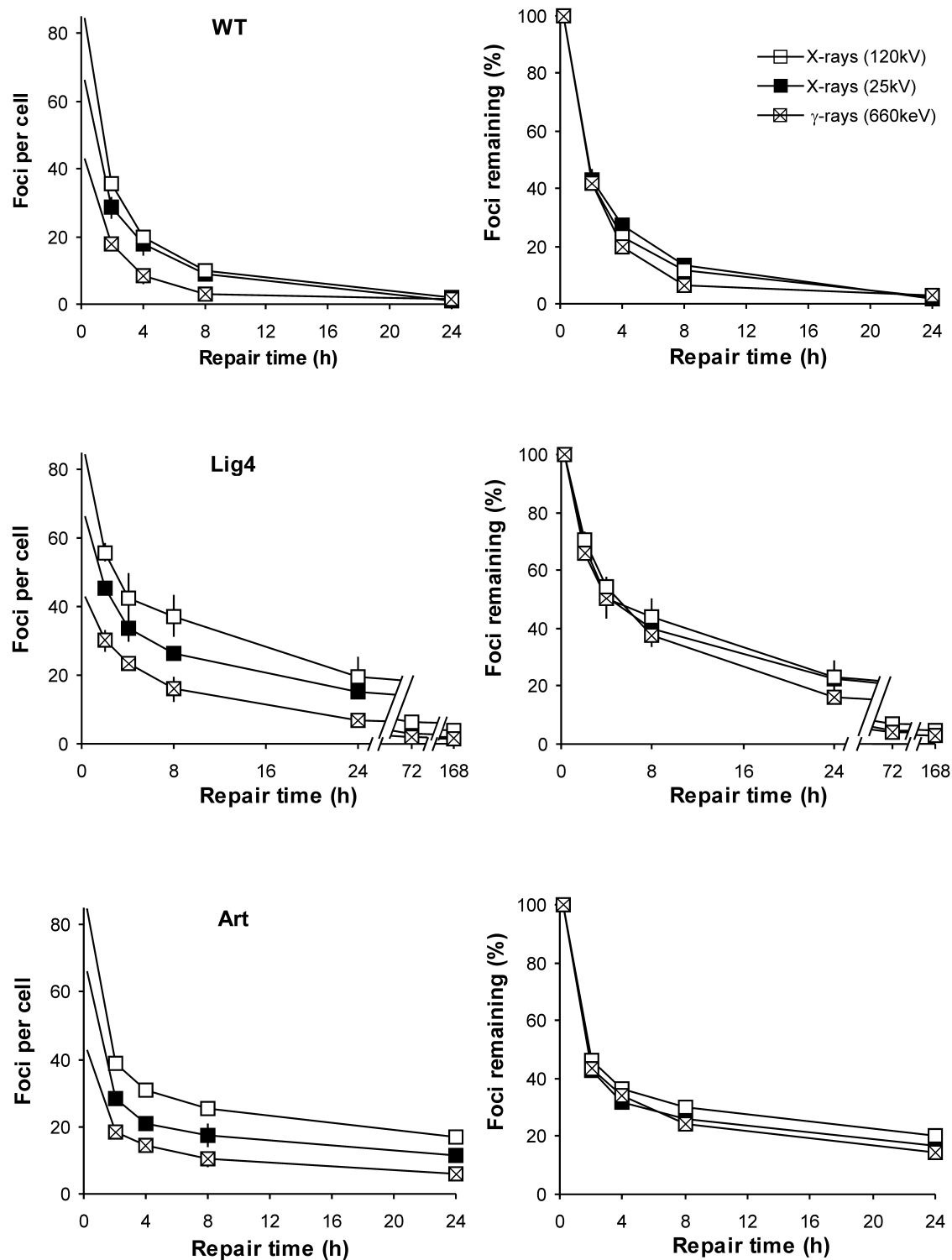


Fig. 3: Kinetics for the loss of  $\gamma$ H2AX foci assessed at various times post irradiation with 2 Gy in primary human fibroblasts grown on glass coverslips (WT: MRC-5 control cells; Lig4: DNA ligase IV defective 180BR cells; Art: Artemis defective F01-240 cells). Left panels: Foci numbers per cell. Right panels: Percentage of foci remaining. These values were obtained by dividing the foci numbers at different time points by the foci numbers at 15 min. The latter numbers were calculated from the induction yield obtained in Fig. 1 for the three different radiation qualities. Error bars represent the SE from at least 3 independent experiments.

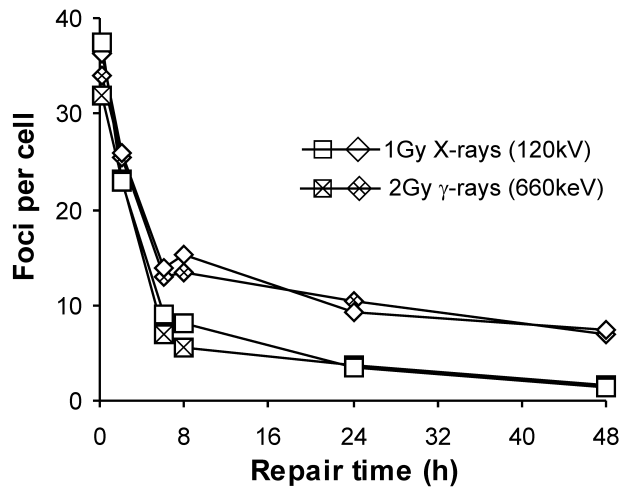


Fig. 4: Kinetics for the loss of  $\gamma$ H2AX foci assessed at various times post irradiation with 1 Gy 120 kV X-rays or 2 Gy  $\gamma$ -rays in hTert immortalized human fibroblasts grown on glass coverslips (squares: 48BRhTert control cells; diamonds: Artemis defective CJ179hTert cells). 1 Gy 120 kV X-rays and 2 Gy  $\gamma$ -rays provide similar numbers of foci per cell at all analysed time points, demonstrating a two-fold higher induction yield for X-rays relative to  $\gamma$ -rays but similar kinetics of foci loss for both radiation qualities. Data represent results from a single experiment.